NANO LETTERS

Letter

pubs.acs.org/NanoLett

Microfluidic Fabrication of Colloidal Nanomaterials-Encapsulated Microcapsules for Biomolecular Sensing

Xi Xie,[†,‡,§] Weixia Zhang,[#] Alireza Abbaspourrad,[#,▽] Jiyoung Ahn,[∥] Andrew Bader,[‡] Suman Bose,[‡,§] Arturo Vegas,[‡,§] Jiaqi Lin,[‡,§] Jun Tao,[†] Tian Hang,[†] Hyomin Lee,[#] Nicole Iverson,[∥] Gili Bisker,[∥] Linxian Li,[‡,§] Michael S. Strano,[∥] David A. Weitz,[#] and Daniel G. Anderson[*,‡,§,○,⊥]

[†]The First Affiliated Hospital, School of Electronics and Information Technology, Sun Yat-Sen University, Guangzhou 510275, China

[‡]David H. Koch Institute for Integrative Cancer Research, [§]Department of Chemical Engineering, [∥]Department of Chemical Engineering, and [⊥]Harvard MIT Division of Health Sciences and Technology, Massachusetts Institute of Technology, Cambridge, Massachusetts 02139, United States

[#]School of Engineering and Applied Sciences, Department of Physics, Harvard University, Cambridge, Massachusetts 02138, United States

[▽]Department of Food Science, Cornell University, Ithaca, New York 14853, United States

[○]Institute for Medical Engineering and Science, Massachusetts Institute of Technology, Cambridge, Massachusetts 02139, United States

Supporting Information

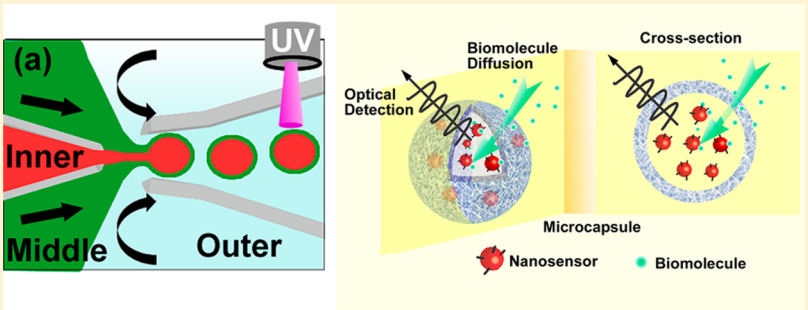

ABSTRACT: Implantable sensors that detect biomarkers in vivo are critical for early disease diagnostics. Although many colloidal nanomaterials have been developed into optical sensors to detect biomolecules in vitro, their application in vivo as implantable sensors is hindered by potential migration or clearance from the implantation site. One potential solution is incorporating colloidal nanosensors in hydrogel scaffold prior to implantation. However, direct contact between the nanosensors and hydrogel matrix has the potential to disrupt sensor performance. Here, we develop a hollow-microcapsule-based sensing platform that protects colloidal nanosensors from direct contact with hydrogel matrix. Using microfluidics, colloidal nanosensors were encapsulated in polyethylene glycol microcapsules with liquid cores. The microcapsules selectively trap the nanosensors within the core while allowing free diffusion of smaller molecules such as glucose and heparin. Glucose-responsive quantum dots or gold nanorods or heparin-responsive gold nanorods were each encapsulated. Microcapsules loaded with these sensors showed responsive optical signals in the presence of target biomolecules (glucose or heparin). Furthermore, these microcapsules can be immobilized into biocompatible hydrogel as implantable devices for biomolecular sensing. This technique offers new opportunities to extend the utility of colloidal nanosensors from solution-based detection to implantable device-based detection.

KEYWORDS: *Microcapsules, microfluidic fabrication, nanosensors, biomolecular sensing*

Point-of care systems and personalized medical devices require implantable sensors that are able to continuously detect and monitor analytes in vivo so that disease can be detected for early diagnosis or real-time monitoring.[1,2] Advances in nanomaterial-based sensors have the potential to substantially improve disease diagnoses.[3−6] In particular, many types of colloidal nanoparticles,[7−11] nanorods,[3,12] carbon nanotubes,[4] and graphene[13] have been investigated as optical sensors. Many of these nanosensors exhibit different types of optical changes in response to a variety of cues such as fluorescence lifetime,[14] spectrum,[3,15] and polarization.[16] To achieve specificity in these responses, nanomaterials have been conjugated to ligands that provide specific binding of analytes. Upon target binding, the nanosensors generate[15,17] or amplify[18,19] an optical responses. Some examples of previously

Received: January 3, 2017
Revised: January 27, 2017
Published: February 3, 2017

DOI: 10.1021/acs.nanolett.7b00026
Nano Lett. XXXX, XXX, XXX−XXX

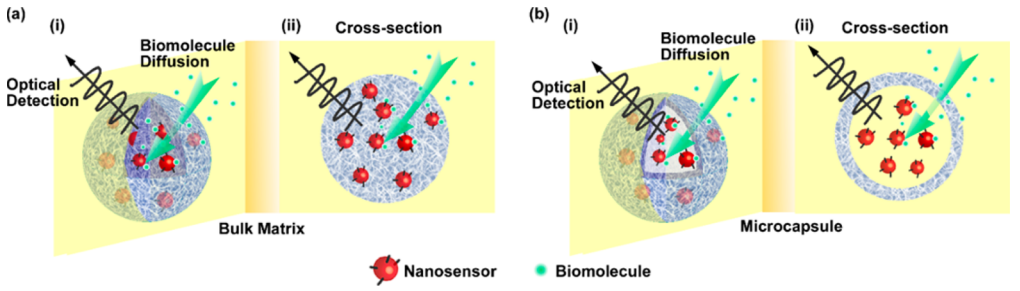

Figure 1. (a) Colloidal nanosensors in bulk hydrogel matrix. Direct contact of colloidal nanosensors with the hydrogel matrix has the potential to impact sensor activity. (b) Colloidal nanosensors encapsulated in microcapsules with a liquid core. The nanosensors were sealed in the microcapsules but freely disperse throughout the internal liquid core. Biomolecules can diffuse through the polymer matrix freely and interact with the trapped nanosensors, generating optical signals to be detected as a result of target biomolecule-sensor binding. Panel ii is the cross-section view of panel i.

studied optical sensing methods include fluorescence,[17] luminescence,[20] and surface-enhanced Raman spectroscopy (SERS)[19] as well as surface plasmon resonance (SPR).[3,15] Biomolecular detection assays using colloidal nanomaterials are generally conducted in vitro, where targeting blood samples or homogenized tissues are added to the aqueous solution of the colloidal nanosensors. Successful applications have been achieved in vitro for the detection of a variety of biomolecules such as glucose,[21−23] heparin,[24] proteins,[25] DNA,[25,26] and ions.[25]

Colloidal nanomaterials must be dispersed in solution phase to function, and in general, two strategies have been implemented to deliver these into the human body. One option is to load colloidal sensors into a dialysis bag and implant the resultant device;[27,28] however, long-term in vivo sensing with these approaches are still limited by biofouling and fibrosis to dialysis materials.[1,28] Another strategy is to incorporate the colloidal nanosensors into a biocompatible hydrogel scaffold (Figure 1a), which can be surgically implanted in human tissue for long-term sensing.[29−31] However, direct contact of colloidal nanosensors with the hydrogel matrix has the potential to impact sensor activity (Supporting Information S1).

Here, we develop colloidal nanosensors encapsulated in microcapsules with a liquid core. The nanosensors were sealed in the microcapsules but freely disperse throughout the internal liquid core (Figure 1b). Biomolecules can diffuse through the polymer shell of the capsules freely and interact with the trapped nanosensors in the core, generating optical signals to be detected as a result of target biomolecule-sensor binding. These capsules can be further coated in a biocompatible hydrogel to create an implantable device for biomolecular sensing.

To demonstrate this design, polyethylene glycol (PEG) microcapsules were fabricated with encapsulated nanosensors using a glass capillary microfluidic technique.[32] Here, we demonstrate that this capsule fabrication methodology can allow for tunable permeability specific to different biomolecules such as glucose, heparin, and streptavidin while retaining encapsulated nanomaterials. In this study, two different functionalized nanosensors, quantum dots (QDs) and gold nanorods (NRs), were successfully encapsulated and utilized to specifically detect biomolecules such as glucose and heparin. These capsules were further immobilized in calcium-alginate hydrogels and retained sensing performance. These results indicate that liquid-core microcapsules may be a versatile and universal platform for encapsulating various colloidal nanosensors for sensing different biomolecules.

Results. A glass capillary microfluidic technique was employed to fabricate template double emulsion droplets (water/oil/water), which were then polymerized to form microcapsules by UV irradiation (Figure 2a).[32] The capillary

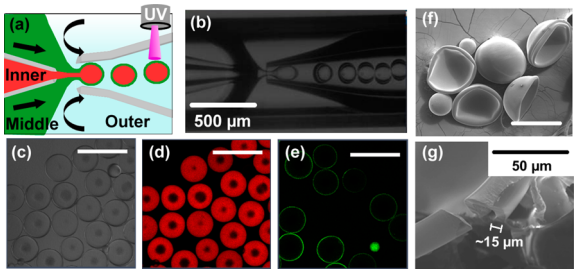

Figure 2. Microcapsules fabrication. (a) Illustration of the capillary microfluidic device for fabrication of microcapsules. The inner (red, water phase containing nanosensors) and middle (green, oil phase containing PEGDA monomer) fluids were focused by the outer (blue, water phase) fluid to generate double emulsion droplets. (b) Optical microscope image showing double emulsion droplet formation. (c) Optical image of the as-fabricated microcapsules. (d) QDs (red) were encapsulated in the capsules. (e) Capsule shells were stained with green fluorescent dye. (f) SEM images of dried microcapsules and (g) the cross-section of the capsule shell was shown. Scale bar: 500 μm in panels c−e and 200 μm in panel f.

microfluidic device was fabricated using three separate capillaries: two tapered cylindrical capillaries, serving, respectively, as injection and collection tubes were inserted and aligned in the third square capillary.[32] An aqueous solution of nanosensors was injected through the injection tube as the inner phase, and a dichloromethane (DCM) solution consisting of 30% (v/v) photocurable monomer, polyethylene glycol diacrylate (PEGDA), and 0.5% (v/v) photoinitiator, 2-hydroxy-2-methyl-1-phenyl-1-propanone, was injected as the middle phase. An aqueous solution containing 10% (w/w) poly(vinyl alcohol) (PVA), which served as surfactant, was injected as the outer phase. It focused the coflowing middle and inner fluids into a fluid thread that then broke into double emulsion drops (Figure 2b), which were further polymerized by UV irradiation to form uniform microcapsules. Some solid beads were generated during the fabrication process due to the rupture of some double emulsion drops before UV irradiation. The microcapsules were washed with water to remove the surfactant and were purified to remove the solid beads based on density difference.

Using this fabrication method, 5 nm diameter red fluorescent CdSe/ZnS quantum dots (emission wavelength of ~655 nm)

DOI: 10.1021/acs.nanolett.7b00026
Nano Lett. XXXX, XXX, XXX−XXX

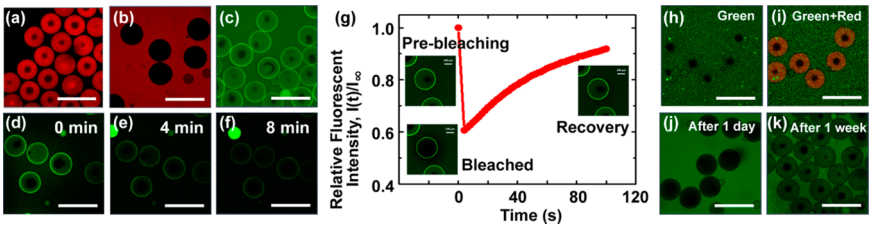

Figure 3. Confocal fluorescence images showing the PEG capsule permeability to QDs and different biomolecules. (a) Capsules loaded with QDs (red) were stable over 1 month. (b) QDs (red) were not able to diffuse into the microcapsules after the capsules were incubated with QD solution for 1 month. (c) The microcapsules were permeable to glucose analog (green fluorescence). (d–f) Real-time fluorescence images showing glucose analog (green fluorescence) trapped inside the capsules were able to freely diffuse to the outer medium. (g) FRAP experiment to determine the capsule permeation to glucose analog. (h,i) The QDs-loaded capsules (red) were permeable to heparin-FITC (green) within 1 h. (j) Streptavidin-FITC has limited diffusion into the capsules after incubation for 1 day. (k) Extended incubation of the capsules with streptavidin-FITC for 1 week leaded to the permeation of streptavidin into the capsules eventually. Scale bar: 500 μm in panels a–f and h–k.

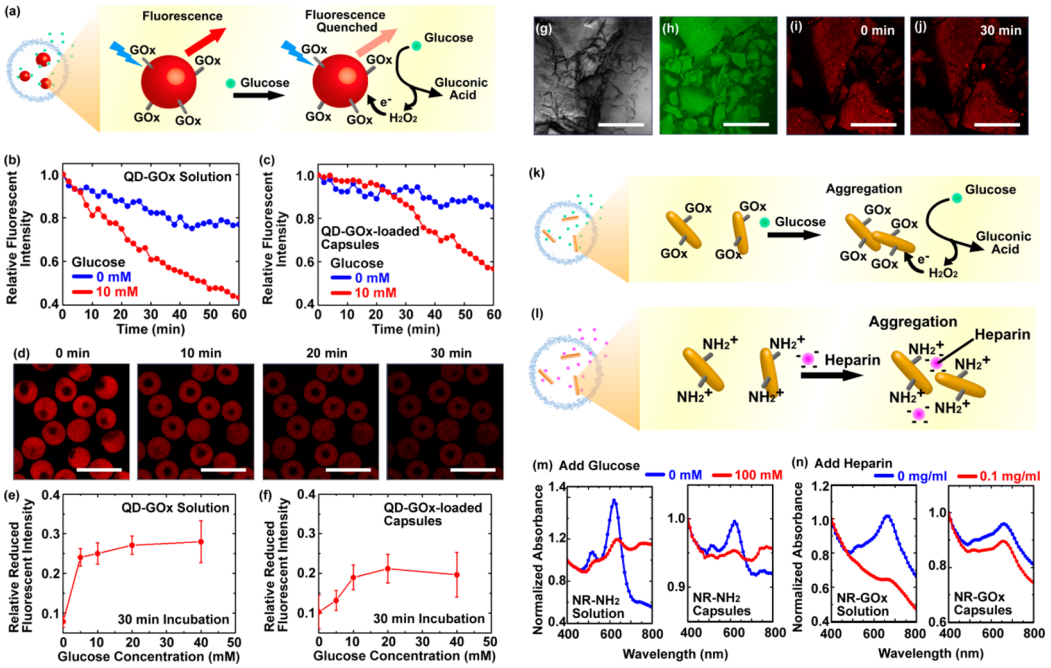

Figure 4. (a–f) The glucose sensing application of microcapsules loaded with QD-GOx nanosensors. (a) Schematic illustration of the QD-GOx glucose nanosensors. (b,c) The fluorescence intensity of QD-GOx decreases with reaction time when 10 mM glucose was added to the (a) QD-GOx solution or the (b) QD-GOx-loaded capsules. (d) Real-time (0–30 min) confocal fluorescence images showing the fluorescence of the QD-GOx loaded capsules was quenched when they were exposed to 10 mM glucose solution. (e) The QD-GOx solution and (f) the QD-GOx-loaded capsules were used to detect a series of glucose solutions of different concentration. Error bar indicates standard deviation of the mean (N = 3). (g) Optical images of PEG hydrogel powders. (h) Glucose analog (green fluorescence) was able to diffuse freely into the PEG hydrogel matrix within 10 min. (i) QD-GOx (red fluorescence) were dispersed in the PEG hydrogel. Glucose solution (1000 mM) was added to the hydrogel (j) but induced little change on the fluorescence intensity of the QD-GOx. (k) Schematic illustration of the gold NR-GOx glucose nanosensors. (l) Schematic illustration of the gold NR-NH_2 heparin nanosensors. (m) The SPR band changing of the NR-GOx solution and the NR-GOx-loaded capsules after exposure to 100 mM glucose for 6 h. (n) The SPR band changing of the NR-NH_2 solution and the NR-NH_2-loaded capsules after exposure to 0.1 mg/mL heparin for 3 h. Scale bar: 500 μm in panels d and g–j.

were encapsulated in the inner phase of PEG capsules. As shown by optical image in the Figure 2c, the diameter of the resultant capsules were ~250 μm. Confocal fluorescence microscopy imaging indicates that the QDs were successfully encapsulated and dispersed in the liquid cores (Figure 2d). It should be noted that the PEGDA monomer used is water-soluble and, hence, may diffuse into the inner phase (water) from the middle phase (DCM). These PEGDA monomers were then cross-linked by UV irradiation, forming some condensed PEG polymer in the liquid core of the capsules, which resulted in the dark spots observed in the liquid cores as seen in the confocal fluorescence images (Supporting Information S2). In Figure 2e, the shells of the capsules were stained with fluorescein isothiocyanate (FITC), a green fluorescent dye. To prepare samples for imaging in scanning electron microscopy (SEM), the capsules were dried under ambient conditions. After drying, the collapsed capsules (Figure 2f) were sliced to determine the thickness of the capsule shells, which were found to be ~15 μm (Figure 2g).

The capsules were stable, and >99% remained intact over one month (Figures 3a and S3). The permeation of QDs into the interior of the capsules was studied by using a confocal fluorescence microscopy to evaluate whether QDs can diffuse into capsules. Instead of encapsulating the QDs inside the capsules, an aqueous solution of QDs was added from the top medium to the capsules whose liquid cores initially only

DOI: 10.1021/acs.nanolett.7b00026
Nano Lett. XXXX, XXX, XXX–XXX

contained water without any QDs (Figure S3). The QDs were not able to diffuse into the capsules, as the interiors of the capsules remained dark even after exposed to the QDs solution for one month (Figure 3b). Only a few of the capsules (<0.1%) ruptured leading to QDs diffusion into their interiors (Figure S3). These results indicate that the PEG shell of the capsule can prevent the QDs from diffusing through the capsule boundary, demonstrating that QDs can be encapsulated inside the capsules without leaking out.

The permeation of biomolecules into the interior of the capsules was determined by exposing the capsules to the aqueous solution of biomolecules (Figure S4). To test the permeation to glucose molecule (MW ≈ 180 Da), a fluorescent glucose analog, 2-(*N*-(7-nitrobenz-2-oxa-1,3-diazol-4-yl)-Amino)-2-deoxyglucose (2-NBDG, MW ≈ 342 Da) was used for these studies.[33] As shown by the results in Figure 3c, fluorescent intensity of the interior of the capsules was as bright as the outer aqueous phase after 2-NBDG was added to the capsules for 1 min, which suggests the fluorescent glucose analog can diffuse freely through the capsule shells (Figure S5). In reverse, if the outer fluorescent medium was removed and replaced with phosphate-buffered saline (PBS) solution that contained no glucose analog, the fluorescent intensity was initially brighter inside the capsules (Figure 3d) but rapidly decreased to the similar intensity level as the outer medium within 10 min (Figures 3e,f and S5). This result suggests that the glucose analog trapped inside the capsules can readily diffuse through the capsule shell to the outer medium. In addition, the capsule permeability was demonstrated via fluorescence recovery after photobleaching (FRAP).[34] In this experiment, glucose analog was allowed to diffuse into the capsules, and then the interior region of a capsule was exposed to an intensive laser pulse to locally photobleach the glucose analog that was trapped in the capsule. After photobleaching, the unbleached "fresh" glucose analog in the outer medium gradually diffused into the capsule, which resulted in the recovery of interior fluorescence as a function of time (Figure 3g). Based on this fluorescence recovery experiment, the permeability to glucose analog can be calculated to be 1.35 ± 0.25 μm/s (Figure S5).[35]

The capsules' permeability to biomolecules of a larger sizes, such as heparin (MW ≈ 10 kDa, FITC-labeled) and streptavidin (MW ≈ 60 kDa, FITC-labeled), was also determined. As shown in Figure 3h,i, these capsules allowed heparin to diffuse into their interiors within 1 h (Figure S5). However, the streptavidin−FITC protein did not rapidly to diffuse into the capsules after 1 day (Figure 3j). Extended exposure of the capsules to the aqueous solution of streptavidin for 1 week allowed permeation of streptavidin into the capsules (Figure 3k).

To evaluate if these liquid-core capsules can be utilized for biomolecular sensing, several types of nanomaterials (QDs or gold NRs) were made responsive to glucose or heparin and encapsulated in the capsules.[8,22,24,36] The design of QD glucose sensors is based on the strategy developed by Cao et al.,[8] in which glucose oxidase (GOx) was covalently conjugated to the CdSe/ZnS QDs (QD-GOx). The sensing mechanism is based on the fluorescence quenching of CdSe/ZnS QDs by H_2O_2 produced from the GOx-catalyzed oxidation of glucose (Figure 4a). Due to the electron hole traps on QDs serving as the acceptor, the electron-transfer reaction occurs readily when H_2O_2 interacts with the surface of the QDs, leading to the formation of nonfluorescent CdSe anion.[8] The fluorescent intensity of the QD-GOx decreases with reaction time in the presence of glucose (red curve in Figure 4b), and these sensors can detect glucose concentration as low as 1 mM (Figure S6), within the sensitivity range of general glucose sensors for diabetes diagnostics.[27,37]

QD-GOx sensors were encapsulated in the microcapsules as described above. When the capsules were exposed to a 10 mM glucose solution, the fluorescent intensity of the encapsulated QD-GOx decreases with time (red curve in Figure 4c). The real-time images of glucose-induced fluorescence quenching of QD-GOx inside the capsules were shown in Figure 4d. This result indicates that the glucose can readily diffuse into the capsules and was then catalyzed by the GOx on the QDs' surface, producing H_2O_2 that quenched the fluorescence of QDs (Figure S6). In a separate experiment, the QD-GOx solution, or the QD-GOx-loaded capsules interacted with a series of glucose solutions of different concentrations (0, 5, 10, 20, and 40 mM) for a fixed reaction time of 30 min (Figure 4e and 4f). For both QD-GOx solution and the QD-GOx-loaded capsules, the fluorescence intensity decreased as the concentration of glucose increased. For the QD-GOx solution, the relative reduced fluorescence intensity is closely proportional to the concentration of glucose in the range of 0−8 mM (Figure S6) and gradually reaches saturation after concentration >10 mM. For the capsules, the relative reduced fluorescence intensity increased with the increasing glucose concentration up to 20 mM and then reached saturation. These results demonstrate the potential application for these QD-GOx-loaded capsules as a quantitative tool to measure glucose concentration.

To evaluate the importance of dispersing the QD-GOx nanosensors in liquid phase within the capsules, control experiments were conducted by testing the sensing performance of QD-GOx nanosensors dispersed in PEG hydrogel matrix. The capillary microfluidic technique is not suitable to incorporate the nanosensors in solid beads because the nanomaterials have poor dispersity in oil phase such as DCM (Figure S7). Therefore, the QD-GOx nanosensors were directly incorporated in PEG bulk hydrogel by mixing the QD-GOx with 30% (v/v) PEGDA and 0.5% (w/w) photoinitiator, Irgacure 2959, in water, and then the PEGDA was cross-linked via UV irradiation to form hydrogel. The bulk hydrogel was crushed into smaller powders to reduce the distance of mass transportation from outer medium into it.

To test the permeability of the bulk hydrogel or hydrogel powders to biomolecules, fluorescent glucose analog or heparin-FITC was added to them and incubated for 10 min (Figure S7). Fluorescence was observed within the hydrogel from the confocal fluorescence images, which suggests these biomolecules can diffuse into the PEG hydrogel freely (Figure 4g,h). However, the QD-GOx-loaded hydrogel showed limited capability to detect the presence of glucose (Figure S7). The fluorescence of the QD-GOx changed very little over 30 min after 1000 mM glucose was added to the bulk hydrogel or hydrogel powders (Figure 4i,j). These results suggest the sensing performance of QD-GOx was negatively affected due to the direct contact of QD-GOx with PEG polymer, and hence, dispersing the nanosensors in liquid cores of capsules is crucial for maintaining their sensing performance.

To evaluate the utility of this approach with other nanosensors for detecting different biomolecules, in addition to the QD-GOx glucose sensors, another two types of sensors based on gold NRs (length ~40 nm) were tested (Figure 4k,l).

DOI: 10.1021/acs.nanolett.7b00026
Nano Lett. XXXX, XXX, XXX−XXX

In the first example, gold NRs were designed to be responsive to glucose by conjugating NRs with GOx (NR-GOx) according to the method developed by Radhakumary et al. (Figure 4k).[22,36] Glucose can be converted by GOx to produce gluconic acid and H_2O_2 that brings down the ζ potential of the NRs, which induces NRs aggregation and changing of their SPR peak (Figure 4m solution). These NR-GOx sensors were encapsulated in PEG capsules. Although the gold NRs lack visible fluorescence for testing their permeation to the microcapsules, we hypothesized that the capsule shells should prevent the NRs from leaking out because the size of NR is much larger than QDs'. The SPR band changing of the NR-GOx-loaded capsules was shown in Figure 4m capsules, in which the SPR peak (absorbance maxima at 620 nm) of the NR-GOx changed after the capsules were exposed to 100 mM glucose for 6 h.

In a separate experiment, gold NRs were designed to be responsive to heparin by conjugating NRs with amine groups ($NR-NH_2$) based on the technique developed by Cao et al. (Figure 4l),[24] in which the heparin-amine binding induces aggregation of the gold NRs leading to the changing of SPR absorption band (Figure 4n-solution). The SPR band changing of the $NR-NH_2$-loaded capsules was shown in Figure 4n capsules, in which the SPR peak (absorbance maxima at 660 nm) of the NR−GOx became flatter after the capsules were exposed to 0.1 mg/mL heparin for 3 h. These results indicate utility of liquid core microcapsules loaded with different nanosensors for sensing various biomolecules.

Implantation in the body further requires that the surface of the capsule exposed to the body is biocompatible and resistant to biofouling. Toward this end, the QD-GOx-loaded capsules were embedded in calcium alginate hydrogel (Figure 5a), which

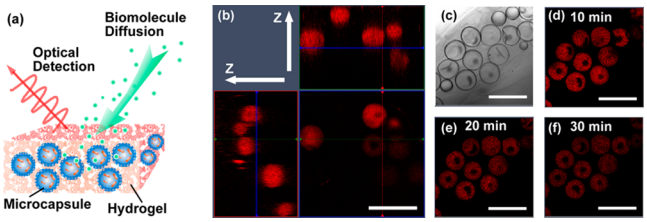

Figure 5. (a) Schematic of the microcapsules immobilized in hydrogel scaffold. Biomolecules are allowed to diffuse through the hydrogel and the capsules to interact with the nanosensors inside the capsules. (b) 3D-converted confocal fluorescence image showing microcapsules (red) were immobilized in Ca^{2+}−alginate hydrogel and distributed at different *Z*-planes. (c) Optical image of capsules embedded in the hydrogel. (d−f) Real-time confocal fluorescence images (at 10, 20, and 30 min) showing the fluorescence of QD-GOx (red) inside the capsules were quenched after 10 mM glucose was added to the hydrogel. Scale bar: 500 μm in panels b−f.

has been previously evaluated in vivo various implantation settings.[38,39] The capsules were initially mixed with an aqueous solution of alginate (1.4%), followed by adding 2.4% Ca^{2+} solution to cross-link the alginate. As shown in the 3D-converted confocal image (Figure 5b), the QD-GOx-loaded capsules (red) distributed at different *Z*-planes within the hydrogel. Glucose analog was able to diffuse freely through the Ca^{2+}-alginate hydrogel into the capsules (Figure S8). When 10 mM glucose was added to this capsule hydrogel, the QD-GOx within the capsule responsively showed reduced fluorescence intensity with increasing reaction time (Figure 5c−f). Therefore, this capsule-loaded hydrogel can demonstrate their function for glucose sensing. In contrast, if the QD-GOx nanosensors were directly loaded in Ca^{2+}-alginate hydrogel, the QD-GOx were loosely trapped in the hydrogel and tended to release to the outer medium over several hours (Figure S9).

Conclusions. In this report, liquid core microcapsules were developed and evaluated for their utility as encapsulation systems for colloidal nanosensors. Microcapsules were fabricated using a capillary microfluidic technique, and colloidal nanomaterials were encapsulated. The microcapsules allow permeation of different biomolecules such as glucose and heparin but prevent the encapsulated nanomaterials inside from leaking out. By encapsulating glucose or heparin-responsive nanosensors, the capsules were able to demonstrate corresponding sensing functionalities. In addition, the microcapsules can be further coated in hydrogels, potentially facilitating their compatibility with the body while preserving sensing function.

The nanosensors-loaded microcapsules developed in this work demonstrate a novel integrated platform to detect biomolecules by utilizing the optical sensing capabilities of colloidal nanomaterials. We expect that a large variety of colloidal nanosensors can be incorporated using this technique for detecting a wide range of biomolecules. As proof of concept, QD and gold NR sensors that only allow one-time sensing were employed in this work, while the using of more sophisticated nanosensors with repeatable detections, fast response, and high sensitivity and with near-infrared spectrum for deeper tissue penetration may enable its use as an implantable sensor for disease management in vivo.

■ ASSOCIATED CONTENT

Supporting Information

The Supporting Information is available free of charge on the ACS Publications website at DOI: 10.1021/acs.nanolett.7b00026.

Additional experimental details, experimental methods, calculation methods, supplemental figures, and supplemental discussion. (PDF)

■ AUTHOR INFORMATION

Corresponding Author

*E-mail: dgander@mit.edu.

ORCID

Xi Xie: 0000-0001-7406-8444
Weixia Zhang: 0000-0002-5835-2020
Hyomin Lee: 0000-0002-0968-431X
Daniel G. Anderson: 0000-0003-0151-4903

Author Contributions

X.X., W.Z., and A.A. contributed equally to this work.

Notes

The authors declare no competing financial interest.

■ ACKNOWLEDGMENTS

The authors thank the MIT Center for Materials Science and Engineering, Microsystems Technology Laboratories, and the W.M Keck Microscopy Facility at the Whitehead Institute for use of equipment and experimental advice. This work was supported by Juvenile Diabetes Research Foundation (JDRF file no. 17-2013-507). The work performed at Harvard was supported by the NSF (DMR-1310266) and the Harvard MRSEC (DMR-1420570). X.X. thanks the Youth 1000 Talents Program and 100 Talents Program of Sun Yat-Sen University (76120-18821104) for supports.

DOI: 10.1021/acs.nanolett.7b00026
Nano Lett. XXXX, XXX, XXX−XXX

REFERENCES

(1) Onuki, Y.; Bhardwaj, U.; Papadimitrakopoulos, F.; Burgess, D. J. *J. Diabetes Sci. Technol.* **2008**, *2*, 1003−1015.
(2) Vaddiraju, S.; Tomazos, I.; Burgess, D. J.; Jain, F. C.; Papadimitrakopoulos, F. *Biosens. Bioelectron.* **2010**, *25*, 1553−1565.
(3) Kabashin, A. V.; Evans, P.; Pastkovsky, S.; Hendren, W.; Wurtz, G. A.; Atkinson, R.; Pollard, R.; Podolskiy, V. A.; Zayats, A. V. *Nat. Mater.* **2009**, *8*, 867−871.
(4) Barone, P. W.; Parker, R. S.; Strano, M. S. *Anal. Chem.* **2005**, *77*, 7556−7562.
(5) Yang, W.; Ratinac, K. R.; Ringer, S. P.; Thordarson, P.; Gooding, J. J.; Braet, F. *Angew. Chem., Int. Ed.* **2010**, *49*, 2114−2138.
(6) Shi, J.; Zhu, Y.; Zhang, X.; Baeyens, W. R. G.; García-Campaña, A. M. *TrAC, Trends Anal. Chem.* **2004**, *23*, 351−360.
(7) Murphy, C. J. *Anal. Chem.* **2002**, *74*, 520−526.
(8) Cao, L.; Ye, J.; Tong, L.; Tang, B. *Chem. - Eur. J.* **2008**, *14*, 9633−9640.
(9) Vilela, D.; González, M. C.; Escarpa, A. *Anal. Chim. Acta* **2012**, *751*, 24−43.
(10) Zhao, W.; Brook, M. A.; Li, Y. *ChemBioChem* **2008**, *9*, 2363−2371.
(11) Slowing, I. I.; Trewyn, B. G.; Giri, S.; Lin, V. S.-Y. *Adv. Funct. Mater.* **2007**, *17*, 1225−1236.
(12) Murphy, C. J.; Gole, A. M.; Hunyadi, S. E.; Stone, J. W.; Sisco, P. N.; Alkilany, A.; Kinard, B. E.; Hankins, P. *Chem. Commun.* **2007**, 544−557.
(13) Morales-Narváez, E.; Merkoçi, A. *Adv. Mater.* **2012**, *24*, 3298−3308.
(14) Medintz, I. L.; Clapp, A. R.; Mattoussi, H.; Goldman, E. R.; Fisher, B.; Mauro, J. M. *Nat. Mater.* **2003**, *2*, 630−638.
(15) Anker, J. N.; Hall, W. P.; Lyandres, O.; Shah, N. C.; Zhao, J.; Van Duyne, R. P. *Nat. Mater.* **2008**, *7*, 442−453.
(16) Huang, Y.; Chen, J.; Shi, M.; Zhao, S.; Chen, Z.-F.; Liang, H. *J. Mater. Chem. B* **2013**, *1*, 2018−2021.
(17) Zhong, W. *Anal. Bioanal. Chem.* **2009**, *394*, 47−59.
(18) Lei, J.; Ju, H. *Chem. Soc. Rev.* **2012**, *41*, 2122−2134.
(19) Tripp, R. A.; Dluhy, R. A.; Zhao, Y. *Nano Today* **2008**, *3*, 31−37.
(20) Wang, L.; Yan, R.; Huo, Z.; Wang, L.; Zeng, J.; Bao, J.; Wang, X.; Peng, Q.; Li, Y. *Angew. Chem., Int. Ed.* **2005**, *44*, 6054−6057.
(21) Barone, P. W.; Strano, M. S. *Angew. Chem., Int. Ed.* **2006**, *45*, 8138−8141.
(22) Radhakumary, C.; Sreenivasan, K. *Anal. Chem.* **2011**, *83*, 2829−2833.
(23) Aslan, K.; Lakowicz, J. R.; Geddes, C. D. *Anal. Biochem.* **2004**, *330*, 145−155.
(24) Cao, R.; Li, B. *Chem. Commun.* **2011**, *47*, 2865−2867.
(25) Xia, F.; Zuo, X.; Yang, R.; Xiao, Y.; Kang, D.; Vallée-Bélisle, A.; Gong, X.; Yuen, J. D.; Hsu, B. B. Y.; Heeger, A. J.; Plaxco, K. W. *Proc. Natl. Acad. Sci. U. S. A.* **2010**, *107*, 10837−10841.
(26) Zhang, J.; Song, S.; Wang, L.; Pan, D.; Fan, C. *Nat. Protoc.* **2007**, *2*, 2888−2895.
(27) Steiner, M.-S.; Duerkop, A.; Wolfbeis, O. S. Optical methods for sensing glucose. *Chem. Soc. Rev.* **2011**, *40*, 4805−4839.
(28) Yum, K.; McNicholas, T. P.; Mu, B.; Strano, M. S. *J. Diabetes Sci. Technol.* **2013**, *7*, 72−87.
(29) Iverson, N. M.; Barone, P. W.; Shandell, M.; Trudel, L. J.; Sen, S.; Sen, F.; Ivanov, V.; Atolia, E.; Farias, E.; McNicholas, T. P.; Reuel, N.; Parry, N. M. A.; Wogan, G. N.; Strano, M. S. *Nat. Nanotechnol.* **2013**, *8*, 873−880.
(30) Balaconis, M. K.; Clark, H. A. *J. Diabetes Sci. Technol.* **2013**, *7*, 53−61.
(31) Kim, S.; Kim, B.; Yadavalli, V. K.; Pishko, M. V. *Anal. Chem.* **2005**, *77*, 6828−6833.
(32) Datta, S. S.; Abbaspourrad, A.; Amstad, E.; Fan, J.; Kim, S.-H.; Romanowsky, M.; Shum, H. C.; Sun, B.; Utada, A. S.; Windbergs, M.; Zhou, S.; Weitz, D. A. *Adv. Mater.* **2014**, *26*, 2205−2218.
(33) Dimitriadis, G.; Maratou, E.; Boutati, E.; Psarra, K.; Papasteriades, C.; Raptis, S. A. *Cytometry, Part A* **2005**, *64*, 27−33.
(34) Lee, D.; Weitz, D. A. *Adv. Mater.* **2008**, *20*, 3498−3503.
(35) Zhihua; Helmuth Möhwald, L. J. *Biomacromolecules* **2006**, *7*, 580−585.
(36) Ren, X.; Yang, L.; Ren, J.; Tang, F. *Nanoscale Res. Lett.* **2010**, *5*, 1658−1663.
(37) Oliver, N. S.; Toumazou, C.; Cass, A. E. G.; Johnston, D. G. *Diabetic Med.* **2009**, *26*, 197−210.
(38) Nunamaker, E. A.; Purcell, E. K.; Kipke, D. R. *J. Biomed. Mater. Res., Part A* **2007**, *83*, 1128−1137.
(39) Orive, G.; Carcaboso, A. M.; Hernández, R. M.; Gascó n, A. R.; Pedraz, J. L. *Biomacromolecules* **2005**, *6*, 927−931.

DOI: 10.1021/acs.nanolett.7b00026
Nano Lett. XXXX, XXX, XXX−XXX